Journal of Anatomy

J. Anat. (2012) **220**, pp29–41 doi: 10.1111/j.1469-7580.2011.01451.x

Relationship between humeral geometry and shoulder muscle power among suspensory, knuckle-walking, and digitigrade/palmigrade quadrupedal primates

Yasuhiro Kikuchi,[1] Hironori Takemoto[2] and Akio Kuraoka[1]

[1]*Division of Human Anatomy and Biological Anthropology, Department of Anatomy and Physiology, Faculty of Medicine, Saga University, Saga, Japan*
[2]*Multimodal Communication Group, Universal Media Research Center, National Institute of Information and Communications Technology, Kyoto, Japan*

Abstract

Shoulder morphology is functionally related to different patterns of locomotion in primates. To investigate this we performed a quantitative analysis of the relationship between cortical bone thickness (Cbt) of the muscle/tendon attachment site on the humerus and physiological cross-sectional area (PCSA) of the shoulder muscle in primates with different locomotory habits. The deltoid, subscapularis, supraspinatus, and infraspinatus were investigated. A chimpanzee, a gibbon, a baboon, two species of macaque, a lutong, a capuchin, and a squirrel monkey were included in the study. The total length of the humerus was measured and the values were converted into three-dimensional reconstructed data on a computer by computed tomography. The Cbt values were obtained from the volumes divided by the areas of the muscle/tendon attachment sites of the humerus by computer analysis. Muscle mass, muscle fascicle length, and muscle pennation angle were measured and PCSA was calculated using these parameters. A relatively high Cbt and small PCSA were characteristic of the gibbon. The gibbon's high Cbt suggests that passive tension in the muscle/tendon attachment site of suspensory primates (brachiators) may be greater than that of quadrupedal primates, whereas the relatively small PCSA indicates an association with a large amount of internal muscle fascia to endure the passive stress of brachiation. Although chimpanzees undertake some suspensory locomotion, the results for this species resemble those of the digitigrade/palmigrade quadrupedal primates rather than those of the suspensory primate. However, the deltoid and subscapularis in chimpanzee differ from those of the other primates and appear to be affected by the peculiar locomotion of knuckle-walking, i.e. the moment arm of forelimb in chimpanzees is relatively longer than that of digitigrade/palmigrade quadrupedal primates. Hence, a large PCSA in the deltoid and subscapularis may contribute to sustaining the body weight during locomotion. On the other hand, a thin cortical bone relative to a large PCSA was a feature of the cercopithecids, indicating that digitigrade/-palmigrade quadrupedal locomotion produces less tension at the muscle/tendon attachment sites compared with that produced by brachiators.

Key words: chimpanzee; computed tomography; cortical bone thickness; gibbon; muscle/tendon attachment site; physiological cross-sectional area.

Introduction

Primates live in various environments and have various types of positional behavior, i.e. terrestrial and arboreal quadrupedalism (digitigrade/palmigrade quadrupedalism), leaping, brachiation, knuckle-walking, and bipedalism (Napier & Napier, 1985; Fleagle, 1999). The shoulder is a part of the body that sensitively reflects differences in morphology functionally associated with different types of locomotion. Therefore, previous studies concerning limb morphology and mechanics have focused on the shoulder. The shoulder muscles have been particularly analyzed to clarify the relationship between mechanical function and locomotion; e.g. muscle mass ratio (Ashton & Oxnard, 1963; Tuttle, 1972; Ashton et al. 1976; Fleagle, 1977; Doyle et al. 1980), interpreted muscle function (Hunt, 1991a),

Correspondence
Yasuhiro Kikuchi, Division of Human Anatomy and Biological Anthropology, Department of Anatomy and Physiology, Faculty of Medicine, Saga University, Saga 849-8501, Japan.
E: kikuchiy@cc.saga-u.ac.jp

Accepted for publication *11 October 2011*
Article published online *4 November 2011*

physiological cross-sectional area (PCSA) (Cheng & Scott, 2000; Anapol & Gray, 2003; Oishi et al. 2009b), muscle fiber type (Singh et al. 2002; Schmidt & Schilling, 2007), and moment arm (Thorpe et al. 1999; Graham & Scott, 2003; Michilsens et al. 2010). Some studies have used electromyographic analysis (Tuttle & Basmajian, 1978a,b; Stern et al. 1980; Larson & Stern, 1986, 1987, 1989, 1992) or cineradiographic analyses (Schmidt & Fischer, 2000; Schmidt, 2005).

In the last decade, muscle morphological analyses in primates have focused on the PCSA in relation to positional behavior or in comparison with human muscle architecture (Anapol & Barry, 1996; Marzke et al. 1999; Thorpe et al. 1999; Cheng & Scott, 2000; Anapol & Gray, 2003; Ogihara et al. 2005; Carlson, 2006; Payne et al. 2006; Oishi et al. 2008, 2009a,b; Channon et al. 2009; Michilsens et al. 2009). Cheng & Scott (2000) reported PCSA in six rhesus macaques (*Macaca mulatta*) and three crab-eating macaques (*Macaca fascicularis*) in the shoulder and elbow muscles. They reported that the two macaque species have quite similar muscle properties despite possessing different brachial indices. Targeting the semi-terrestrial vervets (*Chlorocebus aethiops*) and arboreal red-tailed guenons (*Cercopithecus ascanius*), Anapol & Gray (2003) examined the intrinsic muscles of the shoulder and arm. They concluded that the shoulder and arm muscles of terrestrial vervets have an overall propensity for higher velocity/excursion for rapid terrestrial locomotion compared with those of strictly arboreal red-tailed monkeys. However, they also indicated that the long fibers of the subscapularis and biceps brachii in red-tailed monkeys may produce tension over a broader range of motion. Ogihara et al. (2005) examined internal muscle parameters including PCSA in one chimpanzee forelimb. Carlson (2006) also reported on the fore- and hindlimb muscles in two chimpanzees. Quite recently, hominoid comparative studies have focused on architectural properties and functional interpretations of the upper limb muscles. Oishi et al. (2009b) reported PCSA of three orangutans and four chimpanzees. Their results showed that the subscapularis is significantly larger in orangutans, whereas the infraspinatus is larger in chimpanzees for the rotator cuff muscles, which reflects the functional specialization of their different positional and locomotory behaviors. A similar study was conducted by Michilsens et al. (2009) in gibbons. They emphasized that 'based on this anatomical study, the shoulder flexors, extensors, rotator muscles, elbow flexors and wrist flexors are expected to contribute the most to brachiation'. However, providing only muscle architectural information is insufficient to clarify the detailed morphology associated with positional behavior or mechanical stress during locomotion.

Cortical bone is one of the main structures supporting the body mechanically. The diaphysis of the long bone has relatively thick cortical bone to endure body mass and mechanical stresses. In contrast, the epiphysis has a rather thin cortical bone, and the mechanical stress is absorbed into the trabecular bone, which is structurally similar to a sponge. Therefore, the trabecular bone mainly functions to absorb stress during locomotion. Because the muscles and tendons attach to the surface of the cortical bone, sufficient cortical bone thickness is required to endure the stress produced by muscle contraction. If there is insufficient cortical bone thickness in the proximal humerus at the muscle/tendon attachment site, an avulsion fracture may occur (clinically known: Klasson et al. 1993; Le Huec et al. 1994; Coates & Breidahl, 2001). This observation leads to the hypothesis that the suspensory primates have a cortical bone at the proximal end of the humerus that is relatively thicker and which may experience more stress than that experienced by the cortical bone in quadrupedal primates because not only the muscle contractive stress but also the passive tendon stress affects the muscle/tendon attachment site on the proximal humerus in suspensory animals.

The hypotheses and question of this study are as follows:

- Suspensory primates (brachiators) have a relatively thick cortical bone in the proximal humerus compared with that in the proximal humerus of digitigrade/palmigrade quadrupedal primates, knuckle-walking primates or leaping primates because of passive stress rather than the stress of muscle contraction only. If the suspensory primates do not have sufficient amount of compact bone elements, the proximal humerus might suffer avulsion fracture in the muscle/tendon attachment sites because of excessive mechanical stress.
- Digitigrade/palmigrade quadrupedal primates do not experience passive stress during locomotion, and the muscle/tendon attachment sites on the proximal humerus only experience stress produced by muscle contraction. Therefore, digitigrade/palmigrade quadrupedal primates may have relatively a thinner compact bone than suspensory primates.
- Chimpanzees are knuckle-walkers, but they occasionally use suspensory locomotory activity. Is the cortical bone in chimpanzees thick or thin?

The purpose of this study was to discover how these locomotor repertories affect the muscle/tendon attachment sites on the proximal humerus. Four muscle/tendon attachment sites of the proximal humerus were examined in detail at the level of muscle and cortical bone in the same relative anatomical locations (i.e. deltoid, subscapularis, supraspinatus, and infraspinatus).

Materials and methods

The left shoulder (right shoulder only in the chimpanzee) was investigated in eight subjects (one *Pan troglodytes*, one *Hylobates* sp., one *Papio hamadryas*, one *M. mulatta*, one *M. fascicularis*, one *Trachypithecus francoisi*, one *Cebus albifrons*, and one *Saimiri sciureus* (see Table 1 for common names and abbreviations). The chimpanzee, gibbon, lutong, crab-eating macaque and capuchin monkey were females. The papio and squirrel monkey were males. The gender of the rhesus macaque was

Table 1 Subjects.

	Pan troglodytes	*Hylobates* species	*Papio hamadryas*	*Macaca mulatta*
Sex	F	F	M	Unknown
Body weight (kg)	32.20	[4.93][1]	[20.81][1]	[7.33][1]
Time at death	Adult	Adult	Adult	Adult
English name	Chimpanzee	Gibbon	Baboon	Rhesus macaque
Family	Hominids	Hylobatids	Cercopithecids	Cercopithecids
Frequent locomotor mode	Knuckle-walking[3]	Suspensory (brachiation)[4]	Digitigrade/palmigrade quadrupedalism[5]	Digitigrade/palmigrade quadrupedalism[6]
	Macaca fascicularis	*Trachypithecus francoisi*	*Cebus albifrons*	*Saimiri sciureus*
Sex	F	F	F	M
Body weight (kg)	[4.03][1]	5.08	[2.10][2]	[0.84][2]
Time at death	Adult	Young adult	Adult	Adult
English name	Crab-eating macaque	Lutong	Capuchin monkey	Squirrel monkey
Family	Cercopithecids	Cercopithecids	Cebids	Cebids
Frequent locomotor mode	Digitigrade/palmigrade quadrupedalism[7]	Digitigrade/palmigrade quadrupedalism[8]	Digitigrade/palmigrade quadrupedalism[9]	Digitigrade/palmigrade quadrupedalism[9]

[1]Estimated using humeral head superoinferior breadth according to Ruff (2003).
[2]Estimated using ulnar length according to Anapol & Fleagle (1988).
[3]Hunt (1991a,b, 1992).
[4]Hunt (1991b).
[5]Rose (1977) and Hunt (1991b).
[6]Wells & Turnquist (2001).
[7]Cant (1988).
[8]Workman & Covert (2005).
[9]Johnson & Shapiro (1998).

unknown. The body masses of some individuals were estimated by linear regression previously reported using superoinferior width of humeral head (gibbon, papio, and macaques; Ruff, 2003) and ulnar length (capuchin and squirrel monkeys; Anapol & Fleagle, 1988). Although the ages at death of almost all specimens were unknown, all the specimens were adults or young adult because their humeri had fused at the proximal epiphysis. The chimpanzee was provided by the Chimpanzee Sanctuary Uto, Kumamoto, Japan (Sanwa Kagaku Kenkyusho Co., Ltd) to Saga University. The other cadavers, with the exception of the lutong, were the property of the Department of Anatomy (Macro), Faculty of Medicine, Dokkyo Medical University, Japan. The gibbon, papio, crab-eating macaque, and squirrel monkey were obtained from domestic zoos, and the rhesus macaque from the Laboratory Animal Research Centre of Dokkyo Medical University. The origin of the capuchin was unknown. The lutong was obtained from Itozu Zoo (Kitakyushu, Japan) and was the property of Saga University. The cadavers were soaked for over 3 months in a 10% formalin pool in a laboratory at Saga University. None of the subjects exhibited any disease or deformations of the muscles or bones.

The deltoid, subscapularis, supraspinatus, and infraspinatus as well as the cortical bone thickness (Cbt) at their respective attachment sites on the humerus were examined. The muscles with tendons were removed from the humerus and a black marker gel, which is exposed on X-ray, was placed on the edge of the muscle/tendon attachment sites on the humerus (Fig. 1). After the muscles with tendons had disengaged from the humerus, the muscle mass, muscle fascicle length, and angle of pennation of the muscle fibers (θ) were measured following the methods of Kikuchi (2010a,b). To investigate the inside of the muscle fascicle, the muscle was torn to derive the muscle fascicle length and θ using a digital camera, callipers, and angle gauge (Fig. 2 from Kikuchi, 2010b) (Canon Eos 10D; Canon Inc., Tokyo, Japan; Digimatic; Mitsutoyo Inc., Kanagawa, Japan; Concise Inc., Tokyo, Japan). As superficial fascicles tend to be slightly longer than those within the muscle belly, the superficial fascicles were generally avoided for measurements (Kamibayashi & Richmond, 1998). However, this point is not dealt with in this study because the intraspecific variation of the shoulder muscles almost exceeds the differences between deep and superficial muscle fascicle length, except for small muscles (compared with the results of Kikuchi, 2010a and Kamibayashi & Richmond, 1998). In the broader or larger muscles, three to six different fascicles were measured once each to determine the muscle fascicle length and ensure accuracy. After measuring the muscle fascicle length, the individual muscles were separated into the internal fascia of the origin tendon, the internal fascia/tendon of insertion and the muscle fascicle mass (Fig. 3). The individual muscles were wrapped in pure flannel and compressed until liquid ceased to ooze from them, and muscle mass was measured using an electronic scale (EK.200i; AND Inc., Tokyo, Japan). PCSA was calculated and applied using the measured muscle parameters. PCSA is a good indicator of the force capacities of muscles (Alexander & Vernon, 1975; Zajac, 1989, 1992; Zajac & Gordon, 1989). The formula is as follows:

$$\mathrm{PCSA} = \frac{\mathrm{MM} \times \cos\theta}{\rho \times \mathrm{MFL}}$$

Fig. 1 To clarify the muscle/tendon attachment site on the humerus using CT, a black gel marker, which is exposed on X-ray, was applied to the edge of the muscles/tendon attachment site on the humerus. The black lines (arrow) indicate the gel marks.

where MM is muscle mass, θ is the angle of pennation of the muscle fibers, ρ is muscle density (1.06 g cm^{-3}; Mendez & Keys, 1960) and MFL is muscle fascicle length. If two muscles have the same MM, the muscle with the shorter MFL will have the larger PCSA. A muscle with long fibers has the capacity for high speed and wider excursion but a smaller force potential because of the smaller PCSA (Zajac, 1992).

A three-dimensional (3D) reconstruction technique was applied to obtain the values of Cbt at the muscle/tendon attachment sites of the humerus. A peripheral quantitative computed tomography (CT) machine (XCT 2000 Research+; Norland Stratec Inc., Pforzheim, Germany) was used to obtain 3D images from multiple cross-sectional data of the bone. The specimens were scanned with a scanning resolution of 0.1–0.2 mm per voxel. The beam slice thickness was 0.7 mm, tube voltage was 45–60 kVp, tube current was < 0.3 mA, and CT speed was 7 mm s^{-1}. The slice distance between the individual cross-sectional data was set to the same values as voxel size in order to provide cubic data for each voxels. Cross-sectional raw data were converted into 3D-reconstructed data using software (INTAGE volume editor and AVS EXPRESS; KGT Inc., Tokyo, Japan). Cbt was calculated from the cortical bone area and cortical bone volume data at the muscle/tendon attachment site on the humerus, i.e. the volume divided by the area is equal to the average thickness.

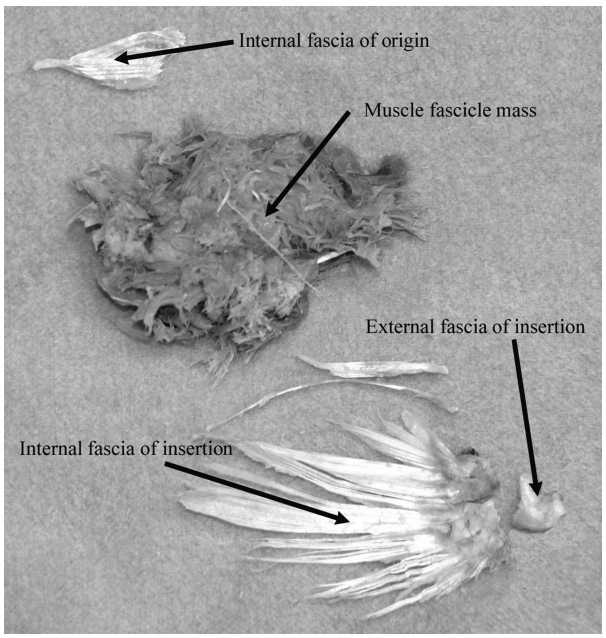

Fig. 3 Image of the subscapularis muscle. Internal fascia at the origin, internal fascia at the insertion, and muscle fascicle mass are separately shown.

The cortical bone area was calculated as follows:

- The threshold of the air and cortical bone surface was set using the half maximum height algorithm (Spoor et al. 1993; Ohman et al. 1997).
- In the individual cross-sectional raw data view for the threshold separating cortical bone and air, the medullary cavity was assigned a value nearly equal to that assigned to the cortical bone element so that only the bone surface could be extracted (Fig. 4).
- The 3D reconstruction technique was applied to create the bone surface and to calculate the cortical bone area. This technique was used to make the minimum number of polygons and iso-surfaces (assembly of a flat surface triangle) between the voxels considering the threshold value between the cortical bone and air (Kono, 2004; Krarup et al. 2005; Tocheri et al. 2005). If the cortical bone surface lacked part of the muscle/tendon attachment site because of a cortical bone density value lower than that of the threshold, the medullary cavity was also assigned a value nearly equal to that assigned to the cortical bone element and the bone surface was carefully contoured to create the original shape; this is

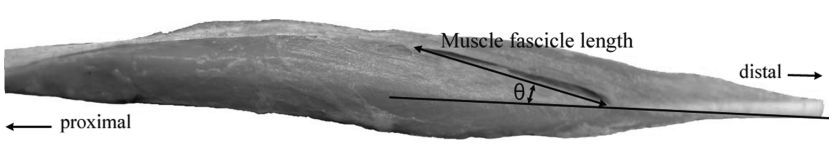

Fig. 2 Image of a muscle indicating muscle fascicle length and θ (reproduced from Kikuchi, 2010b).

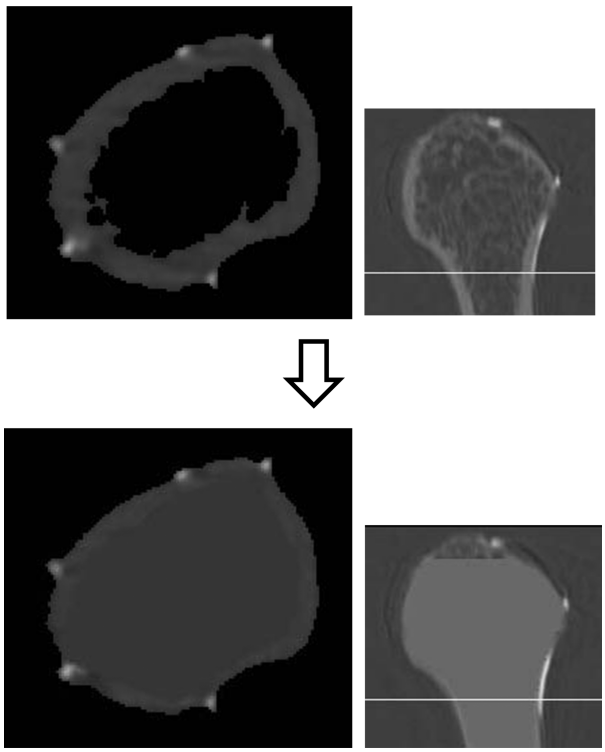

Fig. 4 Cross-sectional raw data. The medullary cavity was assigned a value similar to that assigned to the cortical bone element so that only the bone surface can be extracted. The images on the right indicate the sagittal plane of the humerus and the white lines indicate images on the left.

because a lack of bone surface may lead to an underestimation of the calculated bone area in the 3D reconstructed data. The 3D reconstructed data are shown in Fig. 5.

• Using the 3D reconstructed data, the cortical bone surface of the region of interest (the muscle/tendon attachment site on the humerus) was extracted along with the marker on the X-ray exposed gel (e.g. the deltoid muscle; Fig. 6). The cortical bone surface was trimmed five times to determine the coefficient of variation (CV) in the cortical area, which averaged to 1.3%.

The procedures for calculating the cortical bone volume are as follows:

• The threshold of the air and cortical bone surface was set using the half maximum height algorithm (Spoor et al. 1993; Ohman et al. 1997). The threshold between the cortical bone and trabecular bone was also set using the same algorithm.

• In each cross-sectional raw data view of the threshold separating the cortical bone and trabecular bone, the trabecular bone and bone marrow in the medullary cavity were assigned the value of air (Fig. 7). The cross-section at the threshold separating the cortical bone and air is shown in the lowest panel of Fig. 7, which indicates that the trabecular bone or bone marrow was not inside the bone. If the cortical bone surface was partly lacking the muscle/tendon attachment site because of a cortical bone density value lower than that of the threshold, a similar procedure was performed in the case of area offset. The value near the cortical bone was carefully placed and contoured to make a thin plate (almost one voxel) along the original shape for each cross-sectional raw datum, because a lack of bone surface may lead to an underestimation of calculated bone volume.

• After the cortical bone volume of the region of interest (muscle/tendon attachment site on the humerus) was extracted along the marker on the X-ray exposed gel as the cutting plane was perpendicular to the cortical bone surface (e.g. the deltoid; Fig. 8), the total number of voxels in the region of interest was counted to calculate the volume at a value more than the threshold between the air and cortical bone. Repeatedly trimming the cortical bone five times determined the CV, which averaged 1.4%.

A linear regression analysis was performed between body weight (kg) and the calculated Cbt for each muscle of all the specimens using log-transformed data to verify the calculated Cbt and examine the effect of an offset in case of an underestimation of cortical bone area or volume. If the linear regression was statistically significant, the calculated Cbt was considered valid. PCSAs were then normalized by two-thirds the power of body weight (kg), and Cbts were normalized by one-third the power of body weight (kg). The data were normalized using body weight (kg) and not bone length or bone head diameter

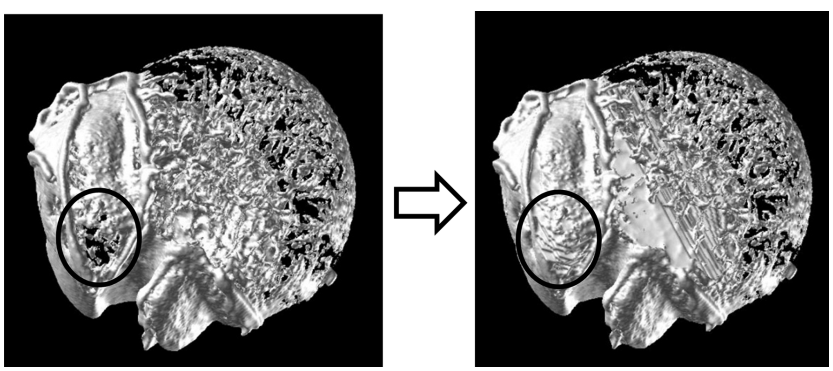

Fig. 5 Cranial view of the proximal humerus. The image to the left indicates that the cortical bone surface of the supraspinatus attachment site was partly lacking. After the medullary cavity was assigned a value nearly equal to that of the cortical bone element and the bone surface was contoured carefully to create the original shape, the data was reconstructed three-dimensionally. The cortical bone surface recovered a thin plate similar to the cortical bone (shown in the right side image).

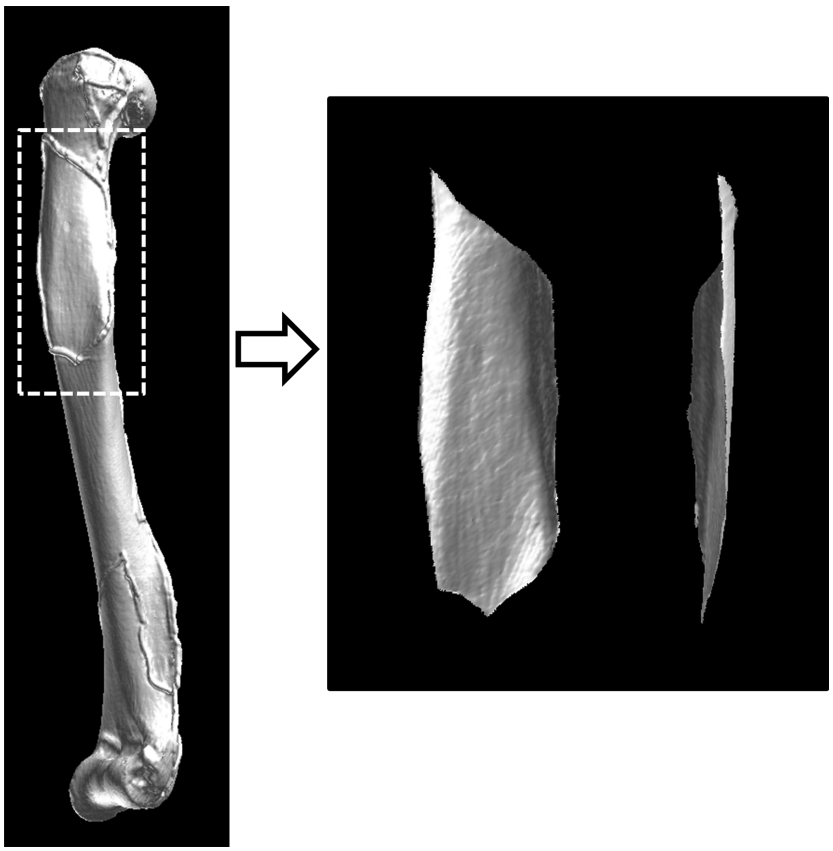

Fig. 6 Using the three-dimensional reconstructed data, the cortical bone surface of the region of interest (the muscle/tendon attachment site) was extracted along the gel marker exposed on X-ray. The image on the right shows the deltoid attachment site on the humerus after trimming.

to take into consideration the body weight endurance of PCSA and Cbt. To clarify the relationship between PCSAs and Cbts of the humeral muscle/tendon attachment site, a point diagram with a least-square regression passing through the origin was applied to individual muscles using Microsoft Office EXCEL 2007. As the numbers of both species and individuals were limited in this study, we analyzed and discussed the characteristics of each primate species.

Limitations of the present study

Regrettably, the living environments of the specimens in the present study were not recorded. However, the wild and captive primates do not differ significantly in terms of bone geometrical properties (lemur; Demes & Jungers, 1993; pig-tailed monkey, Burr et al. 1989; rhesus macaque and crab-eating macaque, Kikuchi, 2009; chimpanzee, Morimoto et al. 2011). Moreover, the intraspecific differences among the different living environments do not exceed the interspecific differences concerning almost all bone geometric properties (Kikuchi, 2009). Although information on the environments where the animals lived is very important, it was unavailable and may be one of the limitations of the present study.

It is necessary to bear in mind that the present study is a preliminary one and has dealt with only one individual per species. To begin addressing this limitation, we calculated intraspecific variation using 10 *M. fascicularis* specimens (Appendix 1) for normalized Cbts, normalized PCSAs (Appendices 2 and 3), weight ratios of the internal fascia of insertion relative to muscle mass, and values concerning the moment arm (MA) (the latter two values are described in the Discussion section; Tables 4 and 5). In the normalized Cbt of the deltoid attachment site, the intraspecific CV exceeds the interspecific CVs in *P. troglodytes* vs. *C. albifrons*, *M. mulatta* vs. *M. fascicularis* and *T. francoisi* vs. *S. sciureus* (Appendix 2). In the normalized PCSA of the deltoid, the intraspecific CV exceeds the interspecific CVs in *Hylobates* sp. vs. *M. fascicularis*, *Hylobates* sp. vs. *T. francoisi*, *P. hamadryas* vs. *M. mulatta*, *M. fascicularis* vs. *T. francoisi*, and *C. albifrons* vs. *S. sciureus.* Regarding the subscapularis, the intraspecific CV of the normalized Cbt exceeds the interspecific CVs in *P. troglodytes* vs. *P. hamadryas*, *Hylobates* sp. vs. *P. hamadryas*, and *M. fascicularis* vs. *S. sciureus.* The intraspecific CV of the normalized PCSA of the subscapularis exceeds the interspecific CVs in *M. mulatta* vs. *T. francoisi* and *M. fascicularis* vs. *S. sciureus.* In the normalized Cbt of the supraspinatus attachment site, the intraspecific CV exceeds the interspecific CVs in *Hylobates* sp. vs. *M. mulatta* and *C. albifrons* vs. *S. sciureus.* (Appendix 3). In the normalized PCSA of the supraspinatus, the intraspecific CV exceeds the interspecific CVs in *P. troglodytes* vs. *M. mulatta*, *P. troglodytes* vs. *M. fascicularis*, *Hylobates* sp. vs. *C. albifrons*, *M. mulatta* vs. *M. fascicularis*, and *C. albifrons* vs. *S. sciureus.* Regarding the infraspinatus, the intraspecific CV of the normalized Cbt exceeds the interspecific CVs in *P. troglodytes* vs. *Hylobates* sp., *P. troglodytes* vs. *P. hamadryas*, *P. troglodytes* vs. *C. albifrons*, *Hylobates* sp. vs. *P. hamadryas*, *Hylobates* sp. vs. *C. albifrons*, *P. hamadryas* vs. *M. mulatta*, *P. hamadryas* vs. *C. albifrons*, and *M. fascicularis* vs. *S. sciureus.* The intraspecific CV of the normalized PCSA of the infraspinatus exceeds the interspecific CVs in *P. troglodytes* vs. *P. hamadryas*, *Hylobates* sp. vs. *C. albifrons*, *M. mulatta* vs. *M. fascicularis*, *M. mulatta* vs. *T. francoisi*, and *M. fascicularis* vs. *T. francoisi* Although the intraspecific CVs in Cbt

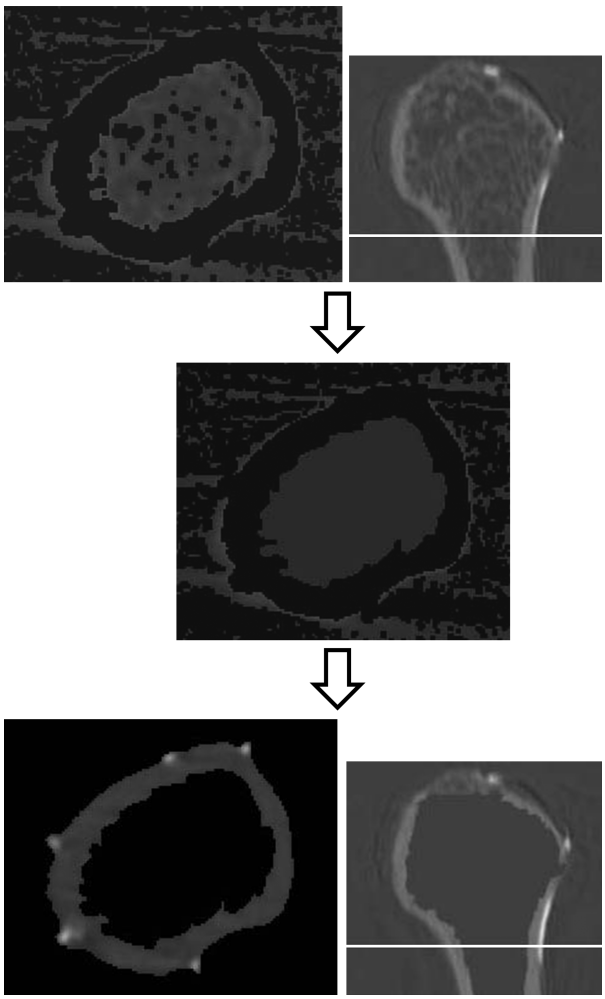

Fig. 7 The top images show that the trabecular bones and bone marrow in the medullary cavity were not removed in the cross-section. The middle image indicates that the trabecular bones and bone marrow in the medullary cavity were assigned the value of air, only cortical bone remaining. The cross-section at the threshold separating the cortical bone and air is shown in the lowest image and indicates that trabecular bone or bone marrow was absent inside the bone. The right side images indicate the sagittal plane of the humerus and the white lines show the positions of the images to the left.

and PCSA values exceeded some of the interspecific CVs, the results of this study were not thought to be limited by intraspecific variation.

Results

The calculated Cbts were considered to be valid because the linear regression analysis between the calculated Cbts and body weight (kg) of each muscle showed a statistically significant relationship ($P < 0.05$) (Table 2). The measured and calculated raw data including Cbt, normalized Cbt, PCSA, normalized PCSA, average muscle fascicle length, muscle mass weight and average cosθ in each muscle are shown in Table 3.

The normalized Cbts of the deltoid and subscapularis in the chimpanzee were much larger than those of other most species (Fig. 9). The normalized PCSAs of the deltoid and subscapularis were the largest in the chimpanzee. The diagram shows a plot positioned near the regression line in the supraspinatus of the chimpanzee. The infraspinatus diagram shows relatively average sizes of the normalized Cbts and the relatively large normalized PCSA in the chimpanzee. The supraspinatus and infraspinatus of the chimpanzee appeared to be similar to those of the cercopithecids.

The normalized Cbt and PCSA of the deltoid in the gibbon were intermediate, whereas the normalized Cbt of the subscapularis was extremely large. However, the gibbon had the smallest normalized subscapularis PCSA among the subjects. The gibbon had a large normalized Cbt and a small normalized PCSA in the supraspinatus compared with those of the other primates. Although the normalized PCSA of the gibbon was small for the infraspinatus, the normalized Cbt was relatively large among the subject species in this muscle. Relatively large normalized Cbts and small normalized PCSAs were observed in the gibbon for all muscles except the deltoid.

The plots of all cercopithecid specimens were positioned near the regression line in the deltoid diagram (Fig. 9). Although the normalized Cbts and PCSAs of the subscapularis showed various values in the cercopithecids, the plots of all cercopithecid specimens were almost near the regression line. The plots of all cercopithecid specimens were above the regression line in the supraspinatus diagram (Fig. 9). The normalized Cbts and PCSAs of the cercopithecids showed various values for the infraspinatus. The positioning of the plots near the regression line was characteristic of the cercopithecids.

The capuchin monkey had an extremely large normalized Cbt and an extremely small normalized PCSA for the deltoid. In the subscapularis, the normalized Cbt showed a medium value, and the normalized PCSA was small. The supraspinatus also had an average normalized Cbt and a small normalized PCSA. The normalized Cbt of the infraspinatus was relatively large. In contrast, the normalized PCSA of the infraspinatus was the smallest compared of all primates examined. Except for the values of the deltoid, the other values of the squirrel monkey were positioned near the regression line (Fig. 9). The deltoid of the squirrel monkey resembled that of the crab-eating macaque and lutong.

Discussion

Electromyographic studies of the shoulder muscles have revealed muscle activity during the support or swing phases of knuckle-walking and pendular suspension in chimpanzees (Larson & Stern, 1986, 1987). According to these reports, in knuckle-walking and pendular suspension, the shoulder muscles (deltoid, subscapularis, supraspinatus, and infraspinatus) are active in both the support and the swing

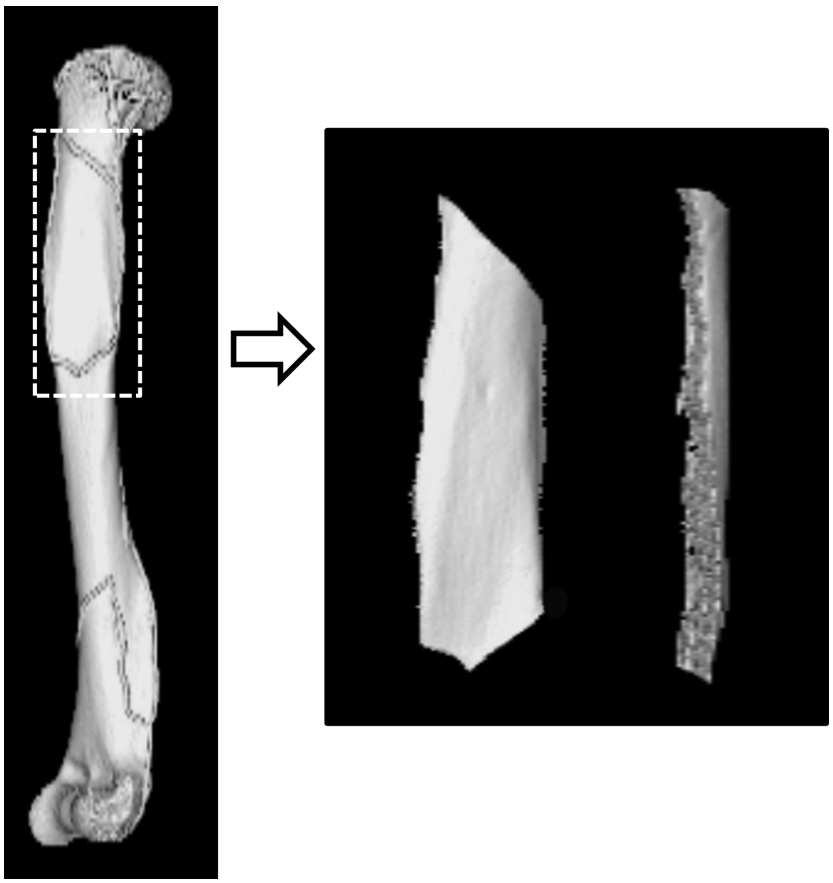

Fig. 8 The cortical bone volume of the region of interest (the muscle/tendon attachment site on the humerus) was extracted along the marker gel exposed on X-ray. The image to the right shows the cut part and the volume data in the deltoid.

Table 2 Result of the linear regression analysis between the calculated Cbts and body weight (kg) of each muscle.

	R	*P*
Deltoid	0.92	< 0.005
Subscapularis	0.88	< 0.005
Supraspinatus	0.80	< 0.05
Infraspinatus	0.85	< 0.01

P, Probability value; *R*, Correlation coefficient.

phase, respectively, despite different activity patterns in each muscle during knuckle-walking and pendular suspension. The results of these studies indicate that the bone–muscle/tendon attachment site always experiences mechanical stress from muscle contraction. Moreover, suspensory primates experience more mechanical stress than non-suspensory primates because of the passive tensile stress at the muscle/tendon attachment site on the humerus; i.e. the humerus experiences mechanical stress, particularly during suspensory locomotion, due not only to muscle contraction but also to passive tension via the tendon or fascia. The larger the passive stress at the muscle/tendon attachment site of the bone, the thicker the Cbt. The present study showed that the suspensory primates (brachiators) experiencing passive mechanical stress have a relatively thick cortical bone at the shoulder muscle/tendon attachment sites on the humerus.

A previous study emphasized that tension forces are exerted on the arms during suspensory locomotion, unlike compressive forces that are exerted during quadrupedal locomotion (Michilsens et al. 2009). According to their report, only the abductor muscles of the shoulder (i.e. deltoid and supraspinatus) have a much lower mass in suspensory primates, i.e. the shoulder abductors have the lowest capacity for power production. That study also indicated that although some compression occurs in the joints because of muscle contraction, the muscles have to work primarily against these gravitational forces to move the body up and forward in suspensory primates. During pendular suspension (brachiation), it is important for shoulder rotator muscles (including the subscapularis and infraspinatus) to stabilize the body to prevent it from swinging mediolaterally rather than forward. Michilsens et al. (2009) reported that the shoulder rotators of gibbons are capable of producing large forces. However, if the passive tension forces are exerted on the muscle/tendon attachment sites on bone, can power generated only by the muscle fibers also counteract the tension forces? If passive stress is larger in suspensory animals than in other primates, the suspensory primates (e.g. brachiators) must have more internal fas-

Table 3 Measured and calculated raw data: cortical bone thickness (Cbt), normalized Cbt, physiological cross-sectional area (PCSA), normalized PCSA, average muscle fascicle length, muscle mass weight and average cos θ.

	Deltoid	Subscapularis	Supraspinatus	Infraspinatus	Deltoid	Subscapularis	Supraspinatus	Infraspinatus
	Cortical bone thickness (Cbt) (cm)				Cbt (normalized)			
Pan troglodytes	0.299	0.128	0.097	0.111	0.094	0.040	0.031	0.035
Hylobates sp.	0.128	0.081	0.045	0.062	0.075	0.048	0.026	0.037
Papio hamadryas	0.225	0.121	0.057	0.118	0.082	0.044	0.021	0.043
Macaca mulatta	0.127	0.062	0.048	0.093	0.065	0.032	0.025	0.048
Macaca fascicularis	0.098	0.033	0.014	0.038	0.061	0.021	0.009	0.024
Trachypithecus francoisi	0.088	0.027	0.011	0.027	0.051	0.016	0.006	0.016
Cebus albifrons	0.123	0.034	0.021	0.048	0.096	0.027	0.016	0.037
Saimiri sciureus	0.050	0.022	0.013	0.020	0.054	0.023	0.014	0.021
	PCSA (cm^2)				PCSA (Normalized)			
Pan troglodytes	29.83	31.69	6.92	9.29	2.95	3.13	0.68	0.92
Hylobates sp.	1.78	1.24	0.64	0.64	0.61	0.43	0.22	0.22
Papio hamadryas	9.07	17.81	6.10	8.06	1.20	2.35	0.81	1.07
Macaca mulatta	4.14	5.65	2.48	2.61	1.10	1.50	0.66	0.69
Macaca fascicularis	1.40	1.89	1.62	1.62	0.55	0.75	0.64	0.64
Trachypithecus francoisi	1.81	4.06	1.23	1.92	0.61	1.37	0.42	0.65
Cebus albifrons	0.50	1.04	0.35	0.33	0.31	0.63	0.21	0.20
Saimiri sciureus	0.28	0.74	0.16	0.31	0.32	0.84	0.19	0.35
	Average muscle fascicle length (cm)				Muscle mass weight (g)			
Pan troglodytes	5.43	2.76	4.06	5.98	180.88	109.85	33.76	62.43
Hylobates sp.	4.31	2.73	2.93	3.20	8.17	3.74	2.25	2.24
Papio hamadryas	6.35	2.89	5.42	5.33	68.87	63.71	39	48.76
Macaca mulatta	4.58	2.45	3.22	3.50	21.92	15.52	9.1	10.29
Macaca fascicularis	3.50	2.26	1.69	1.69	5.64	4.68	3.14	3.14
Trachypithecus francoisi	4.11	2.04	2.45	2.05	9.19	9.00	3.48	4.8
Cebus albifrons	2.94	1.55	1.92	2.28	1.68	1.78	0.75	0.83
Saimiri sciureus	1.87	0.94	1.42	1.53	0.67	0.79	0.26	0.52
	Average cos θ							
Pan troglodytes	0.95	0.84	0.88	0.94				
Hylobates sp.	0.99	0.96	0.88	0.97				
Papio hamadryas	0.89	0.86	0.90	0.93				
Macaca mulatta	0.92	0.95	0.93	0.94				
Macaca fascicularis	0.92	0.97	0.93	0.93				
Trachypithecus francoisi	0.86	0.98	0.92	0.87				
Cebus albifrons	0.93	0.96	0.95	0.96				
Saimiri sciureus	0.84	0.94	0.95	0.96				

cia in the muscle rather than a PCSA that generates muscle power to endure passive tension forces.

The internal fascia mass of insertion relative to the muscle mass was examined in this study (Table 4, Fig. 10). The results showed that the subscapularis, supraspinatus, and infraspinatus of the gibbon had a large internal fascia to muscle ratio. The crab-eating macaque, capuchin monkey, and squirrel monkey also had a relatively high internal fascia to muscle ratio compared with that in other primates. The small-bodied (arboreal) primates tended to have a greater amount of internal fascia compared with that in the large-bodied (terrestrial) primates. This high ratio of internal fascia to muscle may partly contribute to the endurance of passive mechanical stress. The muscles in gibbon and small-bodied (arboreal) primates may be specialized to contain a large amount of internal fascia to endure the mechanical stress during arboreal/suspensory locomotion.

The force-generating capacity of the infraspinatus is higher in chimpanzees, whereas the opposite rotator

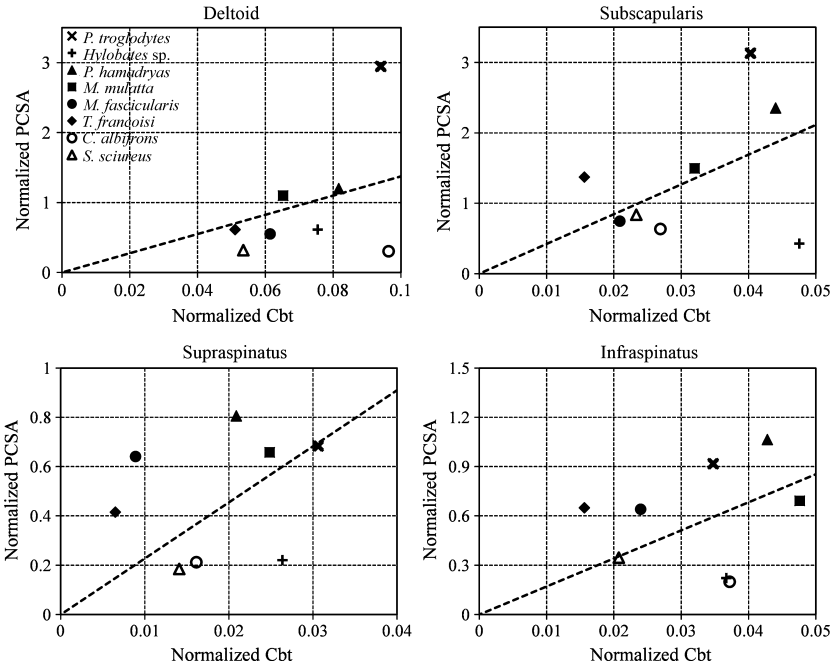

Fig. 9 Diagram of the interrelationship between the normalized Cbt and normalized PCSA of the deltoid, subscapularis, supraspinatus, and infraspinatus. X-mark, the chimpanzee; cross, gibbon; solid triangle, baboon; solid square, rhesus macaque; solid circle, crab-eating macaque; solid diamond, lutong; circle, capuchin monkey; triangle, squirrel monkey. The dotted lines show the least-square regression through the coordinate origin.

Table 4 Ratio of the internal fascia mass of insertion relative to the muscle mass in the subscapularis, supraspinatus, and infraspinatus with the intraspecific coefficient variation (CV) of 10 *Macaca fascicularis* specimens.

	Subscapularis	Supraspinatus	Infraspinatus
Pan troglodytes	0.054	0.075	0.065
Hylobates sp.	0.139	0.093	0.152
Papio hamadryas	0.062	0.045	0.068
Macaca mulatta	0.058	0.043	0.060
Macaca fascicularis	0.120	0.074	0.137
Trachypithecus francoisi	0.054	0.037	0.069
Cebus albifrons	0.129	0.093	0.157
Saimiri sciureus	0.114	0.115	0.115
Intraspecific CV	18.0	12.3	16.8

Intraspecific CV, intraspecific coefficient variation.

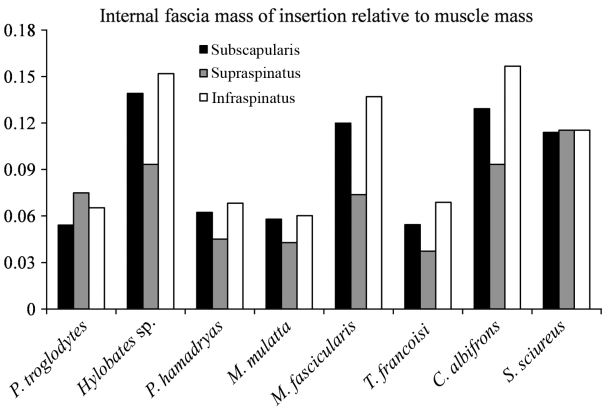

Fig. 10 Weight ratio of the internal fascia of insertion relative to the muscle mass in the subscapularis, supraspinatus, and infraspinatus. Black bar, subscapularis; gray bar, supraspinatus, white bar, infraspinatus.

muscle, the subscapularis, is larger in orangutans (Oishi et al. 2009b). Oishi et al. (2009b) also indicated that the PCSA ratio of the subscapularis is more aligned with the PCSA ratio of the supraspinatus and infraspinatus in the orangutan but that the latter is much larger in chimpanzees. Referring to the work of Larson & Stern (1986, 1987), Oishi et al. (2009b) attributed the small PCSA of the subscapularis in chimpanzees to the observation that these three rotator cuff muscles are active during vertical climbing in the chimpanzee but the subscapularis is not active during knuckle-walking despite the other two muscles being active. They added that functionally specialized morphology for terrestrial adaptation in the chimpanzee was recognized in the rotator cuff muscles.

However, considering muscular and skeletal morphology in this study, the chimpanzee had large Cbts and greater PCSAs in the deltoid and subscapularis, whereas the supraspinatus and infraspinatus of the chimpanzee resembled those of digitigrade/palmigrade quadrupedal monkeys; i.e. the supraspinatus and infraspinatus of the chimpanzee are considered to resemble the muscle power and bone thickness of digitigrade/palmigrade quadrupedal primates. However, the deltoid and subscapularis in the chimpanzee were not similar to those of digitigrade/palmigrade quadrupedal primates. The small subscapularis in chimpanzees compared with that of orangutans (Oishi et al. 2009b) may not necessarily be a particular characteristic of chimpanzees.

The large PCSA of the deltoid and subscapularis may contribute to balance the body because of the relatively longer moment arm of forelimb in chimpanzee than that in the digitigrade/palmigrade quadrupedal primates. Chimpanzees use the power of the deltoid and subscapularis as these muscles have higher potential to support the body and resist larger mechanical stress compared with the digitigrade/palmigrade quadrupedal primates. At the same time, because the chimpanzee uses suspensory locomotion less than knuckle-walking, the shoulder muscles do not require more internal fascia to endure the passive stress (Fig. 10).

The moment arm (MA) was measured to analyze the deltoid (Table 5). Considering the movement and the attachment of the deltoid to the humerus, the MAs of the deltoid were defined as the distance from the midpoint of the humeral head to the middle part of the insertion of the deltoid (similar to Thorpe et al. 1999). Although a clear relationship between PCSAs and MAs was not shown, possibly because of small sample size, the gear ratios devised by Michilsens et al. (2010) clarify the interspecific differences dividing the apes and the non-hominoid primates. The gear ratios were determined by dividing the muscle fascicle length by its mean MA and indicates the ability to move the joint through a certain range of motion (Michilsens et al. 2010). They also stated that 'a muscle with a large gear ratio is able to create substantial moment in a wide range of joint positions, whereas a muscle with a small gear ratio can exert a considerable moment only in a narrow range of joint positions.' In this context, the apes have a deltoid with a large moment and a narrow joint range compared with that of cercopithecids and cebids (Table 5). During both knuckle-walking and brachiation, the shoulder joint requires stability so as not to disarticulate the joint. The deltoid is considered to contribute to shoulder joint stability in both chimpanzees and gibbons despite having different structural mechanics, i.e. different PCSA, different amounts of internal fascia, and different Cbt of the deltoid attachment site.

Jolly (1967) investigated terrestrial quadrupedal locomotion with regard to several features of the postcranial skeleton (referred by Larson & Stern, 1989). One of these features is the proximal prolongation of the greater tubercle of the humerus beyond the profile of the head. He relates this expansion of the greater tubercle to raising the insertion site of the supraspinatus, acting to protract the forelimb and resist passive shoulder extension. In contrast, the non-projecting greater tubercle of more arboreal monkeys is associated with their need for agility, i.e. the short lever arm for the supraspinatus favors fast (though weak) protraction of the humerus in the recovery phase of arboreal quadrupedalism (Jolly, 1967; Larson & Stern, 1989). Apart from the traits of arboreal quadrupedal primates, proximal prolongation of the greater tubercle of the humerus beyond the profile of the head as shown in baboon appears to be one of the reasons why, in the present study, quadrupedal primates (not apes) have a large PCSA and a thin cortical bone. If the muscle/tendon attachment site on the humerus is larger and primates have the same muscle PCSA, the cortical bone may become thinner. The large major tubercle prominent on the humerus appears to connect to the large muscle/tendon attachment site of the supraspinatus. A large muscle/tendon attachment does not need thick cortical bone and leads to thin cortical bone in the humerus. Although a rather faint relationship was found between Cbt and PCSA, and between MA and functional activity among the different species in this study, more accurate analysis and more accumulated data are required.

Table 5 Measured and calculated deltoid values. Humeral length (cm), moment arm (MA) (cm), average muscle fascicle length (cm), PCSA (cm^2), normalized PCSA, normalized MA, and gear ratio with intraspecific coefficient variation (CV) of ten *Macaca fascicularis* specimens. MAs were measured as the distance from the midpoint of the humeral head to the middle part of the insertion of the deltoid. Normalized MAs were calculated as MA divided by humeral length. The gear ratios were determined by dividing the muscle fascicle length by its mean MA (Michilsens et al. 2010).

	Humeral length (cm)	Moment arm (cm)	Average muscle fascicle length (cm)	PCSA (cm^2)	Normalized PCSA	Normalized MA	Gear ratio
P. troglodytes	28.40	8.88	5.43	29.83	2.95	0.31	0.61
Hylobates sp.	22.15	7.16	4.31	1.78	0.61	0.32	0.60
P. hamadryas	22.25	7.82	6.35	9.07	1.20	0.35	0.81
M. mulatta	14.56	4.24	4.58	4.14	1.10	0.29	1.08
M. fascicularis	12.26	3.82	3.50	1.40	0.55	0.31	0.92
T. francoisi	14.19	4.53	4.11	1.81	0.61	0.32	0.91
C. albifrons	9.80	3.04	2.94	0.50	0.31	0.31	0.97
S. sciureus.	7.18	1.82	1.87	0.28	0.32	0.25	1.03
Intraspecific CV	4.52	5.25	6.76	15.10	19.81	3.18	7.58

P. troglodytes, *Pan troglodytes*; *Hylobates* sp., *Hylobates* species; *P. hamadryas*, *Papio hamadryas*; *M. mulatta*, *Macaca mulatta*; *M. fascicularis*, *Macaca fascicularis*; *T. francoisi*, *Trachypithecus francoisi*; *C. albifrons*, *Cebus albifrons*; *S. sciureus.*, *Saimiri sciureus*; intraspecific CV, intraspecific coefficient variation.

Acknowledgements

The authors are extremely grateful to editor-in-chief, Prof. G. M. Morriss-Kay, for reading the proofs of our manuscript. The authors also thank Prof. D. E. Lieberman and two anonymous reviewers for their kind advice and comments regarding this manuscript. Y. Kikuchi thanks the staff of the Chimpanzee Sanctuary Uto, Kumamoto, Japan (Sanwa Kagaku Kenkyusho Co., Ltd) for providing the chimpanzee (with special thanks to Mr. H. Kobayashi and Mr. T. Udono), and the staff at the Itozu Zoo (Kitakyushu, Japan) who kindly provided the lutong. Y. Kikuchi also thanks Dr. M. Yamashita, Dr. H. Takahashi and Mr. H. Sakurai (Department of Anatomy (Macro), Faculty of Medicine, Dokkyo Medical University, Japan) for help in dissecting the primate cadavers. The macaque specimens for clarifying intraspecific variation were kindly provided by the Non-Human Primate Reagent and Resource, Program of the Tsukuba Primate Centre, National Institute of Biomedical Innovation. This study complied with the guidelines of Saga University regarding the ethical treatment of animals, as well as with specific national laws. This study was supported by a MEXT Grant-in-Aid for General Scientific Research (18687017).

References

Alexander RM, Vernon A (1975) The dimensions of knee and ankle muscles and the forces they exert. *J Hum Mov Stud* **1**, 115–123.

Anapol F, Barry K (1996) Fiber architecture of the extensors of the hindlimb in semiterrestrial and arboreal guenons. *Am J Phys Anthrop* **99**, 429–447.

Anapol F, Fleagle JG (1988) Fossil platyrrhine forelimb bones from the early Miocene of Argentina. *Am J Phys Anthrop* **76**, 417–428.

Anapol F, Gray JP (2003) Fiber architecture of the intrinsic muscles of the shoulder and arm in semiterrestrial and arboreal guenons. *Am J Phys Anthrop* **122**, 51–65.

Ashton EH, Oxnard CE (1963) The musculature of the primate shoulder. *Trans Zool Soc London* **29**, 553–650.

Ashton EH, Flinn RM, Oxnard CE, et al. (1976) The adaptation and classificatory significance of certain quantitative features of the forelimb in primates. *J Zool* **179**, 515–556.

Burr DB, Ruff CB, Johnson C (1989) Structural adaptations of the femur and humerus to arboreal and terrestrial environments in 3 species of macaque. *Am J Phys Anthrop* **79**, 357–367.

Cant JG (1988) Positional behavior of long-tailed macaques (*Macaca fascicularis*) in northern Sumatra. *Am J Phys Anthrop* **76**, 29–37.

Carlson KJ (2006) Muscle architecture of the common chimpanzee (*Pan troglodytes*): perspectives for investigating chimpanzee behavior. *Primates* **47**, 218–229.

Channon AJ, Günther MM, Crompton RH, et al. (2009) Mechanical constraints on the functional morphology of the gibbon hind limb. *J Anat* **215**, 383–400.

Cheng EJ, Scott SH (2000) Morphometry of *Macaca mulatta* forelimb. I. Shoulder and elbow muscles and segment inertial parameters. *J Morphol* **245**, 206–224.

Coates MH, Breidahl W (2001) Humeral avulsion of the anterior band of the inferior glenohumeral ligament with associated subscapularis bony avulsion in skeletally immature patients. *Skeletal Radiol* **30**, 661–666.

Demes B, Jungers WL (1993) Long-bone cross-sectional dimensoins, locomotor adaptations and body-size in prosimian primates. *J Hum Evol* **25**, 57–74.

Doyle WJ, Siegel MI, Kimes KR (1980) Scapular correlates of muscle morphology in *Macaca mulatta*. *Acta Anat* **106**, 493–501.

Fleagle JG (1977) Locomotor behavior and muscular anatomy of sympatric Malaysian leaf-monkeys (*Presbytis obscura* and *Presbytis melalophos*). *Am J Phys Anthrop* **46**, 297–307.

Fleagle JG (1999) Chapter 3: primate lives, locomotion. In: *Primate Adaptation and Evolution*, 2nd edn (ed. Fleagle JG), pp. 57–57. San Diego: Academic Press.

Graham KM, Scott SH (2003) Morphometry of *Macaca mulatta* forelimb. III. Moment arm of shoulder and elbow muscles. *J Morphol* **255**, 301–314.

Hunt KD (1991a) Mechanical implications of chimpanzee positional behavior. *Am J Phys Anthrop* **86**, 521–536.

Hunt KD (1991b) Positional behavior in the Hominoidea. *Int J Primatol* **12**, 95–118.

Hunt KD (1992) Positional behavior of *Pan troglodytes* in the Mahale Mountains and Gombe Stream National Parks, Tanzania. *Am J Phys Anthrop* **87**, 83–105.

Johnson SE, Shapiro LJ (1998) Positional behavior and vertebral morphology in atelines and cebines. *Am J Phys Anthrop* **105**, 333–354.

Jolly CJ (1967) The evolution of the baboons. In: *The Baboon in Medical Research*, Vol 2. (ed. Vagborg H), pp. 23–50. Austin: University of Texas Press.

Kamibayashi LK, Richmond FJ (1998) Morphology of human neck muscles. *Spine* **23**, 1314–1323.

Kikuchi Y, Hamada Y (2009) Geometric characters of the radius and tibia in *Macaca mulatta* and *Macaca fascicularis*. *Primates* **50**, 169–183.

Kikuchi Y (2010a) Quantitative analysis of variation in muscle internal parameters in crab-eating macaques (*Macaca fascicularis*). *Anthropol Sci* **118**, 9–21.

Kikuchi Y (2010b) Comparative analysis of muscle architecture in primate arm and forearm. *Anat Histol Embryol* **39**, 93–106.

Klasson SC, Vander Schilden JL, Park JP (1993) Late effect of isolated avulsion fractures of the lesser tubercle of the humerus in children. Report of two cases. *J Bone Joint Surg Am* **75**, 1691–1694.

Kono RT (2004) Molar enamel thickness and distribution patterns in extant great apes and humans: new insights based on a 3-dimensional whole crown perspective. *Anthropol Sci* **112**, 121–146.

Krarup S, Darvann TA, Larsen P, et al. (2005) Three-dimensional analysis of mandibular growth and tooth eruption. *J Anat* **207**, 669–682.

Larson SG, Stern JT Jr (1986) EMG of scapulohumeral muscles in the chimpanzee during reaching and 'arboreal' locomotion. *Am J Anat* **176**, 171–190.

Larson SG, Stern JT Jr (1987) EMG of chimpanzee shoulder muscles during knuckle-walking: problems of terrestrial locomotion in a suspensory adapted primate. *J Zool Lond* **212**, 629–655.

Larson SG, Stern JT Jr (1989) Role of supraspinatus in the quadrupedal locomotion of vervets (*Cercopithecus aethiops*): implications for interpretation of humeral morphology. *Am J Phys Anthrop* **79**, 369–377.

Larson SG, Stern JT Jr (1992) Further evidence for the role of supraspinatus in quadrupedal monkeys. *Am J Phys Anthrop* **87**, 359–363.

Le Huec JC, Schaeverbeke T, Moinard M, et al. (1994) Isolated avulsion fracture of the lesser tubercle of the humerus in children. *Acta Orthop Belg* **60**, 427–429.

Marzke MW, Marzke RF, Linscheid RL, et al. (1999) Chimpanzee thumb muscle cross-sections, moment arms and potential torques, and comparisons with humans. *Am J Phys Anthropol* **110**, 163–178.

Mendez J, Keys A (1960) Density and composition of mammalian muscle. *Metabolism* **9**, 184–188.

Michilsens F, Vereecke EE, D'Août K, et al. (2009) Functional anatomy of the gibbon forelimb: adaptation to a brachiating lifestyle. *J Anat* **215**, 335–354.

Michilsens F, Vereecke EE, D'Août K, et al. (2010) Muscle moment arms and function of the siamang forelimb during brachiation. *J Anat* **217**, 521–535.

Morimoto N, Ponce De León MS, Zollikofer CPE (2011) Exploring femoral diaphyseal shape variation in wild and captive chimpanzees by means of morphometric mapping: a test of Wolff's law. *Anat Rec* **294**, 589–609.

Napier JR, Napier PH (eds) (1985) Chapter 3: structure and function, locomotion. In: *The Natural History of the Primates. Massachusetts*. pp. 44–55. Cambridge: The MIT Press.

Ogihara N, Kunai T, Nakatsukasa M (2005) Muscle dimensions in the chimpanzee hand. *Primates* **46**, 275–280.

Ohman JC, Krochta TJ, Lovejoy CO, et al. (1997) Cortical bone distribution in the femoral neck of hominoids: implication for the locomotion of *Australopithecus afarensis*. *Am J Phys Anthropol* **104**, 117–131.

Oishi M, Ogihara N, Endo H, et al. (2008) Muscle architecture of the upper limb in the orangutan. *Primates* **49**, 204–209.

Oishi M, Ogihara N, Endo H, et al. (2009a) Dimensions of the foot muscles in the lowland gorilla. *J Vet Med Sci* **71**, 821–824.

Oishi M, Ogihara N, Endo H, et al. (2009b) Dimensions of forelimb muscles in orangutans and chimpanzees. *J Anat* **215**, 373–382.

Payne RC, Crompton RH, Isler K, et al. (2006) Morphological analysis of the hindlimb in apes and humans. I. Muscle architecture. *J Anat* **208**, 709–724.

Rose MD (1977) Positional behaviour of live baboons (*Papio anubis*) and its relationship to maintenance and social activities. *Primates* **18**, 59–116.

Ruff CB (2003) Long bone articular and diaphyseal structure in Old World monkeys and apes. II: Estimation of body mass. *Am J Phys Anthropol* **120**, 16–37.

Schmidt M (2005) Quadrupedal locomotion in squirrel monkeys (Cebidae: *S. sciureus*): a cineradiographic study of limb kinematics and related substrate reaction forces. *Am J Phys Anthrop* **128**, 359–370.

Schmidt M, Fischer MS (2000) Cineradiographic study of forelimb movements during quadrupedal walking in the brown lemur (*Eulemur fulvus*, Primates: *Lemuridae*). *Am J Phys Anthrop* **111**, 245–262.

Schmidt M, Schilling N (2007) Fiber type distribution in the shoulder muscles of the tree shrew, the cotton-top tamarin, and the squirrel monkey related to shoulder movements and forelimb loading. *J Hum Evol* **52**, 401–419.

Singh K, Melis EH, Richmond FJ, et al. (2002) Morphometry of *Macaca mulatta* forelimb. II. Fiber-type composition in shoulder and elbow muscles. *J Morphol* **251**, 323–332.

Spoor CF, Zonneveld FW, Macho GA (1993) Linear measurements of cortical bone and dental enamel by computed tomography: applications and problems. *Am J Phys Anthrop* **91**, 469–484.

Stern JT Jr, Wells JP, Jungers WL, et al. (1980) An electromyographic study of the pectoralis major in atelines and *Hylobates*, with special reference to the evolution of a pars clavicularis. *Am J Phys Anthrop* **52**, 13–25.

Thorpe SK, Crompton RH, Günther MM, et al. (1999) Dimensions and moment arms of the hind- and forelimb muscles of common chimpanzees (*Pan troglodytes*). *Am J Phys Anthrop* **110**, 179–199.

Tocheri MW, Razdan A, Williams RC, et al. (2005) A 3D quantitative comparison of trapezium and trapezoid relative articular and nonarticular surface areas in modern humans and great apes. *J Hum Evol* **49**, 570–586.

Tuttle RH (1972) Functional and evolutionary biology of hylobatid hands and feet. *Gibbon and Siamang* **1**, 136–206.

Tuttle RH, Basmajian JV (1978a) Electromyography of pongid shoulder muscles. II. Deltoid, rhomboid and 'rotator cuff'. *Am J Phys Anthrop* **49**, 47–56.

Tuttle RH, Basmajian JV (1978b) Electromyography of pongid shoulder muscles. III. Quadrupedal positional behavior. *Am J Phys Anthrop* **49**, 57–70.

Wells JP, Turnquist JE (2001) Ontogeny of locomotion in rhesus macaques (*Macaca mulatta*): II. Postural and locomotor behavior and habitat use in a free ranging colony. *Am J Phys Anthrop* **115**, 80–94.

Workman C, Covert HH (2005) Learning the ropes: the ontogeny of locomotion in red-shanked douc (*Pygathrix nemaeus*), Delacour's (*Trachypithecus delacouri*), and Hatinh langurs (*Trachypithecus hatinhensis*). I. Positional behavior. *Am J Phys Anthrop* **128**, 371–380.

Zajac FE (1989) Muscle and tendon: properties, models, scaling, and application to biomechanics and motor control. *Crit Rev Biomed Eng* **17**, 359–411.

Zajac FE (1992) How musculotendon architecture and joint geometry affect the capacity of muscles to move and exert force on objects: a review with application to arm and forearm tendon transfer design. *J Hand Surg Am* **17**, 799–804.

Zajac FE, Gordon ME (1989) Determining muscle's force and action in multi-articular movement. *Exerc Sport Sci Rev* **17**, 187–230.

Supporting Information

Additional Supporting Information may be found in the online version of this article:

Appendix S1. Data from *Macaca fascicularis* specimens for clarifying intraspecific variation.

Appendix S2. Intraspecific coefficient variation (CV) of 10 *Macaca fascicularis* specimens and interspecific differences are indicated as percentages (%) for the normalized Cbt and normalized PCSA of the deltoid and subscapularis.

Appendix S3. Intraspecific coefficient variation (CV) of 10 *Macaca fascicularis* specimens and interspecific differences are indicated as percentages (%) for the normalized Cbt and normalized PCSA in the supraspinatus and infraspinatus.

As a service to our authors and readers, this journal provides supporting information supplied by the authors. Such materials are peer-reviewed and may be re-organized for online delivery, but are not copy-edited or typeset. Technical support issues arising from supporting information (other than missing files) should be addressed to the authors.